Synthesis of Soluble and Highly Thermally Stable Polyaniline- Titanium Dioxide Composite via Inverse Emulsion Polymerization

[1]Anwar-ul-Haq Ali Shah, [1]Saima Shaheen, [1]Muhammad Kamran, [1]Humaira Seema
[2]Rizwan Ullah and [2]Salma Bilal*
[1]*Institute of Chemical Sciences, University of Peshawar, 25120, Pakistan.*
[2]*National Center of Excellence in Physical Chemistry, University of Peshawar, Pakistan.*
salmabilal@uop.edu.pk*

(Received on 2nd February 2018, accepted in revised form 20th December 2018)

Summary: Polyaniline (PANI)/Titanium dioxide (TiO_2) composites were prepared by polymerization of aniline in the presence of TiO_2 using inverse emulsion polymerization protocol. In this method 2-butanol and chloroform were used as dispersing media and the materials were tested for corrosion protection of stainless steel in Indian Ocean water. The amount of aniline, oxidant (Benzoyl peroxide), Dodecylbenzenesulphonic acid (DBSA) surfactant and metal oxide (TiO_2) were varied in the reaction bath for optimum yield. The as-synthesized PANI and PANI-TiO_2 composites were soluble in a number of common organic solvents and characterized with Ultravilot-visivble (UV-Vis) and Fourier Transform Infra-Red (FT-IR) spectroscopies. The surface morphology, particle size and crystinality were determined with Scanning Electron Microscopy (SEM) and X-Rays Diffraction (XRD) analysis. Thermogravimetric analysis (TGA) was employed to determine thermal stability of the composite. The total mass loss was found to be 58% in PANI as compared to 22% in PANI-TiO_2 showing comparatively higher thermal stability of the composites. The composites were electrochemically active in acidic medium and reduced corrosion rate of steel to 0.9083 mm/ year Indian Ocean water. Finally it was concluded that PANI-TiO_2 composites could be employed as anticorrosive coatings for steel in aggressive corrosive environment

Keywords: PANI-TiO_2, Composite, Inverse emulsion polymerization, Corrosion.

Introduction

Polyaniline (PANI) is considered as one of the most promising member of conducting polymers family due to high electrical conductivity, ease of synthesis, remarkable redox properties and good environmental stability [1-3]. The role of PANI and its derivatives has been acknowledged in a wide range of applications such as solar cells [4, 5], electrochromic devices [6, 7], electromagnetic interface shielding [8, 9] and rechargeable batteries [10-12]. However, low process ability, fragile nature and chemical instability render the applications of polyaniline [13]. Attempts have been made to improve mechanical strength, thermal, environmental and chemical stability of PANI by making its composites with metals and metal oxides [14, 15]. Mostly synergic effect of PANI composites with particular metal/metal oxides has been reported for the enhancement of performance of a specific property in polyaniline by making silver (PANI/Ag) [16, 17], polyaniline –gold (PANI/Au) [18, 19], PANI/TiO_2 [20, 21] and PANI/C [22, 23] composites.

The composite of PANI with TiO_2 is appealing for further research because of low cost, non-toxicity, excellent optical properties and stability of TiO_2 towards photochemical corrosion. TiO_2 is an n-type semiconductor [24] and usually used for the detection of gases like NO_2, H_2 and NH_3. However, some of its applications are limited by its wide band gap. The conduction band of TiO_2 matches very well with the lowest unoccupied molecular orbital (LUMO) of polyaniline. At the interfaces electric transport properties such as charge carrier mobility are expected to increase during chemical interaction between PANI and TiO_2[25] in their composites. PANI/TiO_2 has been used in corrosion protection coating for steel [26], gas-sensitivity [21], and fuel cell [20].

Various protocols such as *in situ* polymerization [27-28], sol-gel [29] and ultrasonic irradiation [30] have been reported for the preparation of PANI/ metal oxide composites. But the preparation of conducting polymers based composites via inverse emulsion polymerization, where monomer, oxidant and protonic acid are mixed with water and non-polar solvent [31] in the presence of metal oxide has drawn the attention of many researchers [32, 33]. Due to physical state of emulsion system it is easy to control the process and the product can be used directly without further separations in many cases [34]. The surface area available for polymerization reaction is very high in this method which increases the contact rate among monomer, dopant and the oxidant. The synthesis of pristine PANI by inverse emulsion polymerization

*To whom all correspondence should be addressed.

has already been reported. However, to the best of our knowledge there is no report on the preparation of PANI/TiO_2 composite via inverse emulsion polymerization.

In this work the synthesis of PANI/TiO_2 composite is reported for the first time by inverse emulsion polymerization pathway. The PANI and PANI/TiO_2 composites were prepared by using chloroform and 2-butanol as a dispersing medium, benzoyl peroxide as oxidant, DBSA as surfactant and water as inorganic medium. The effect of concentration of aniline, benzoyl peroxide, DBSA and TiO_2 on the % yield was investigated. The as-synthesized PANI and PANI-TiO_2 composites were soluble in a number of common organic solvents like a mixture of toluene and 2-propanol, dimethyl sulfoxide (DMSO) and chloroform ($CHCl_3$). The composites were characterized with UV-Vis & FT-IR spectroscopy, Scanning Electron Microscopy (SEM), X-Rays Diffraction (XRD) and Thermogravimetric analysis (TGA). The composites were electrochemically active in acidic medium and applied for corrosion protection of steel in Indian Ocean water.

Experimental

Materials

Aniline was purchased from Acros and stored under nitrogen atmosphere in a refrigerator after vacuum distillation. All other chemicals were analytical grade and used as received. TiO_2 powder was purchased from BDH with particle size 200-300 nm, 2-butanol (Aldrich), chloroform (Scharlau), Dodecylbenzenesulphonic acid (Acros), 2-propanol (Merck), benzoyl peroxide (Merck) and toluene (Scharlau)

Measurements

For characterization of the composites Ultraviolet-visible (UV-vis) spectrometer Perkin Elmer (UK), Fourier Transform Infrared (FTIR) spectrometer Shimadzu, IRPrestige-21 and Scanning Electron microscope (SEM) JEOL, JSM-6490 was used. Thermogravimetric analysis was carried out by Perkin Elmer, Diamond series (USA) with a heating rate of 10°/min in N_2 atmosphere. Cyclic voltammograms were recorded with a Gamry Reference 3000 workstation in a three electrode setup. For this purpose PANI and PANI-TiO_2 was drop coated on the gold sheet electrode and used as working electrode after drying. A gold wire and saturated calomel electrodes were used as counter and reference electrodes respectively. Cyclic voltammograms were recorded in 0.5 M H_2SO_4 solution in the potential of -0.2 to 0.85V at 50 mV/s scan rate. Conductivity of the synthesized PANI and PANI-TiO_2 composites was measured with four probe conductivity setup on pressed pellets with Jandel RM3000 test unit (UK).

The corrosion protection properties of PANI and PANI-TiO_2 were studied on stainless steel in Indian Ocean water by using three electrode single compartment cell. Stainless steel disc, saturated calomel and platinum electrodes were used as working, reference and counter electrodes, respectively. Stainless steel disc was polished against an abrasive paper and washed with acetone, ethanol and distilled water to remove any impurities. Samples were dissolved in mixture of chloroform and 2-propanol, coated on stainless steel by drop coating method and dried at room temperature for 30 minutes. The potentiodynamic current density/potential curve or Tafel plot was obtained by using Gamry Reference 3000 workstation. DC105 DC Corrosion software was used to evaluate corrosion parameters. The tafel curve was extrapolated and values of corrosion potential (E_{corr}), corrosion current (i_{corr}) and corrosion rate (CR mm/year) were determined by using GamryEchem analyst software.

Synthesis

Inverse emulsion polymerization of monomers was carried out for the preparation PANI-TiO_2 composites with various compositions by addition of TiO_2 particles. In a typical method 0.29 mol of chloroform was taken in a 100 mL round bottom flask under constant stirring, followed by the addition of 1.25 mmol of benzoyl peroxide. To the above solution 0.13 mol of 2-butanol, 3.73 mmol of DBSA and 1.07 mmol of aniline were added step wise. 1.017 mmol of titanium dioxide powder sonicated for 10 min at room temperature in 0.28 mol of distilled water was then added to the above mixture for the formation of a milky white emulsion. The reaction mixture turned green after 5 h continuous stirring. However, the reaction was continued for 24 h for maximum conversion of the reagents into the composites. Finally the organic phase was separated and washed repeatedly with acetone and plenty of water. The resulting green film of the composites was broken in to flakes by the addition of a very small amount of acetone. For comparison pristine PANI was also synthesized by the same method without addition of TiO_2 powder.

Following formula [35] was used for percent yield calculation.

$$\% \text{ Yield} = \frac{Weight of PANI - TiO_2}{\textbf{Weight of Aniline} + \textbf{Weight of } TiO_2} \times 100$$

Results and Discussion

Percent Yield

The concentrations of monomer, oxidant and TiO_2 have marked effect on % yield of the product. The effect of monomer concentration on the % yield was studied by varying aniline concentration in the feed (Fig 1a). No product formation was observed with very low concentration of aniline (4.3×10^{-4} mol). Step wise increase in the concentration of aniline resulted in the increase of product formation. Maximum product formation was observed at 1.09 mmol of aniline. Beyond 1.09 mmol of aniline the decrease in the product formation is attributed to the rapid decrease in efficiency of oxidant with the increase in monomer concentration[36].

The effect of oxidant concentration on the product formation is depicted in Fig 1b. Maximum product formation was observed with 1.25 mmol of benzoyl peroxide. The decrease in the yield beyond 1.25 mmol of benzoyl peroxide may be due to over oxidation that causes the decomposition of the polymer chains in the composite[33].

The effect of concentration of DBSA on the % yield is depicted in Fig.1c. The % yield increases with the increase in concentration of DBSA upto 3.73 mmol. Beyond this concentration the product formation decreases which is attributed to the formation of excessive emulsion particles that reduces monomer diffusion to the surface of emulsion particles. As a result the chain growth gets restricted with reduction in molecular weight. More oligomers were formed that could be run off quickly while washing the polymer composite with acetone [33].

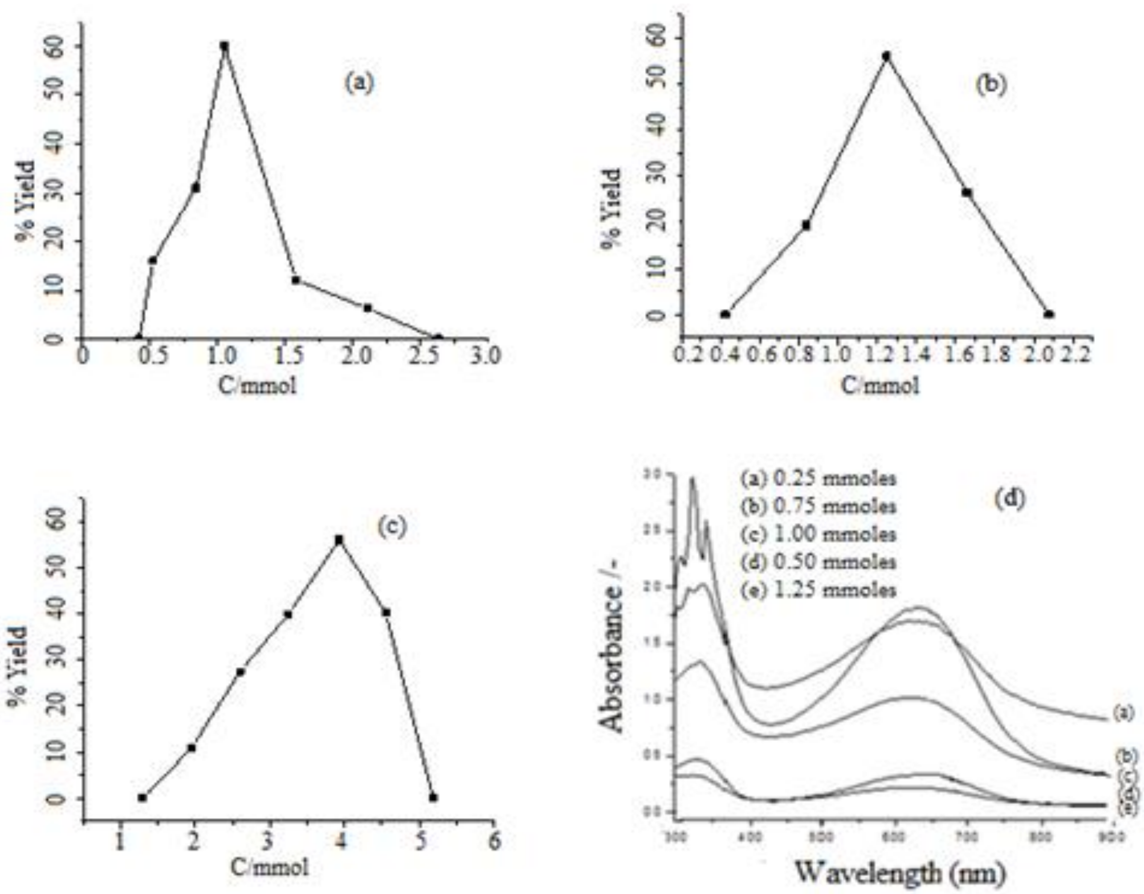

Fig. 1: Effect of a)monomerb)oxidant c) DBSA concentration on % yield and d) UV-Vis spectra of synthesized composites with different concentration of TiO_2.

Different amounts of TiO_2 (Table-1) were introduced into the reaction vessel for the preparation of PANI-TiO_2 composites. UV-vis spectral results in the Table-1 and Fig 1d indicate that in the absence of TiO_2, PANI shows two electronic absorption bands at 335 and 640 nm which were blue shifted due to the presence of metal oxide (TiO_2) particles. The different interaction of TiO_2 with PANI decreases the overlapping between lone pair of nitrogen and π electrons of phenyl ring that results in changes in the peak positions [37]. The maximum blue shifting of the peak from 640 to 619 nm was observed at 1.0017×10^{-3} mol of TiO_2. Based on the above observation it is concluded that maximum yield of the composite is obtained with 3.73, 1.09, 1.25 and 1.0017 mmol of DBSA, aniline, benzoyl peroxide and TiO_2 respectively.

Table-1: UV-Vis spectral bands of PANI& PANI-TiO_2 composites.

S.NO	Conc. of TiO_2 (mol)	Name of Sample	UV-Vis bands
1.	0	PANI	640,340
2.	1.25×10^{-3}	$PANIT_1$	625,335
3.	1.0017×10^{-3}	$PANIT_2$	619,335
4.	7.5×10^{-4}	$PANIT_3$	630,335
5.	5.0×10^{-4}	$PANIT_4$	640, 335

Solubility

Solubility is an important aspect of conducting polymers and their composite materials. It is considered very crucial for application of these fascinating materials which would otherwise be very difficult to cast on any substrate for onwards use. The solubility of PANI-TiO_2 was checked in a number of solvents as depicted in Fig 2 which demonstrates that the composite prepared in the present study is soluble in chloroform, 2:1 mixture of toluene & 2-propanol and dimethyl sulfoxide. This is attributed to the incorporation of DBSA into PANI chain. The solubility is facilitated by the long alkyl chain of DBSA in common organic solvents[38].

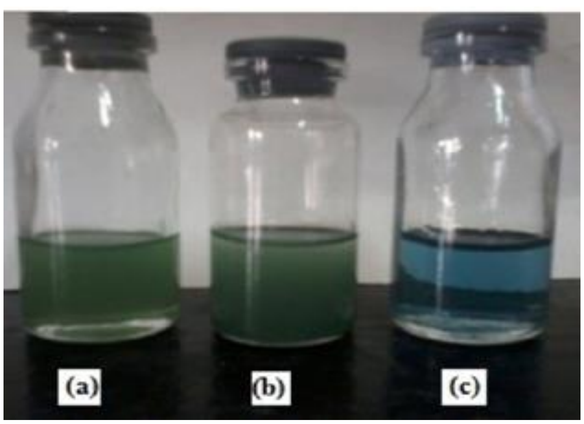

Fig. 2: Solution of PANI-TiO_2composite in (a) chloroform, (b) 2:1 mixture of toluene + 2-propanol, and(c) DMSO.

UV-Vis Spectroscopy

UV-vis spectroscopy is commonly used to identify the type of electronic transition as well as the extent of doping in conducting polymers and their composites with other materials. UV-vis spectra of PANI and PANI-TiO_2 composite in *N*-methylpyrrolidinone are shown in Fig. 3. The two bands at 335 and 640 nm in the electronic absorption spectrum of PANI are associated with π-π* transition of benzoid rings and n-π*transition of quinoid rings (polaron transition)[39] respectively. UV-vis spectrum of PANI-TiO_2 composite displays the same feature as that of PANI. However, the band associated with n-π*transition is observed at 619 nm. The spectra of both PANI and its composite with TiO_2 reflect doped nature of the material as already reported in PANI-DBSA salt. The blue shifting of 21 nm is due to the interaction of TiO_2 particles with PANI, which decreases the degree of orbital overlapping between the π electrons of the phenyl rings with loan pair of nitrogen atom. Subsequently the peaks were shifted as a result of decrease in conjugation of polyaniline [40]. This also shows the dedoping of PANI-DBSA salt to some extent because in the composite some of the DBSA molecules are replaced by TiO_2 particles.

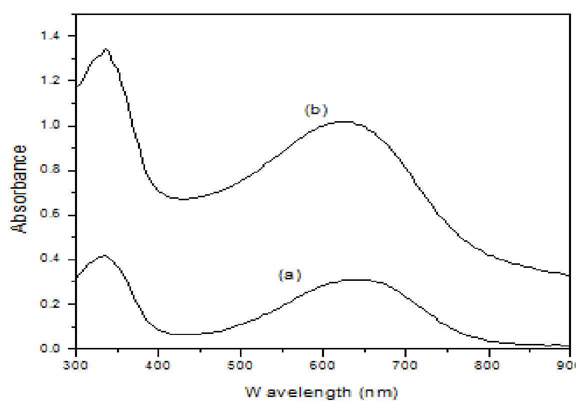

Fig. 3: UV–Vis spectra of (a) PANI-DBSA salt and (b) PANI-TiO_2 composite recorded in *N*-methylpyrrolidinone solution

Scanning Electron Microscopy

Fig. 4 (a-d) shows low and high magnification scanning electron microscopic (SEM) images of bulk PANI-DBSA salt and PANI- TiO_2 composite. It is observed that both PANI and its composite exhibit granular morphology. The appearance of globular or granular morphology is due to presence of phenazine containing nucleates which aggregates randomly and start the growth of polymer chain in star burst way [41, 42]. The mean particle size of PANI is about 0.36 µm while that of PANI-TiO_2 is 0.40 µm which shows the insertion of TiO_2 into polymer chain. Both PANI and PANI-TiO_2 composite have a very porous structure and a lot of micropores have been observed in the micrographs of composite. This microporous nature of PANI-TiO_2 increases liquid-solid interfacial area for the extraction and insertion of gas molecules which makes it a suitable candidate for the gas sensing [43].

X-Rays Diffraction Study

X-Rays Diffraction study (XRD) is widely employed for the identification of materials. It is a non-destructive technique and is used for the analysis of microcrystalline and powder samples. XRD patterns of PANI-TiO_2, TiO_2 and PANI are shown in Fig 5. The patterns were recorded in a range of 10-80º. The PANI powder showed three broad peaks at 2θ angles of 14.44º, 16.77º and 27.85º respectively. This crystallinity of the material is indicated by the sharp and well defined peaks [28]. These peaks may be attributed to the scattering from the perpendicular periodicity at the interplaner spacing of the PANI chains[28]. XRD pattern of pure TiO_2 showed peaks appearing at 25º, 37.75º, 48.23º, 54.06º, 55.43º and 62.61º which are in accordance with literature [25, 44]. Additional diffraction peaks appeared at 2θ values of 38.9º, 48.23º, 54º, 55.6º and 63.19º for PANI-TiO_2 composite associated with the presence of TiO_2 particles [45]. The appearance of sharp peaks due to the insertion of TiO_2 might have increased the crystallinity of the resulting composite.

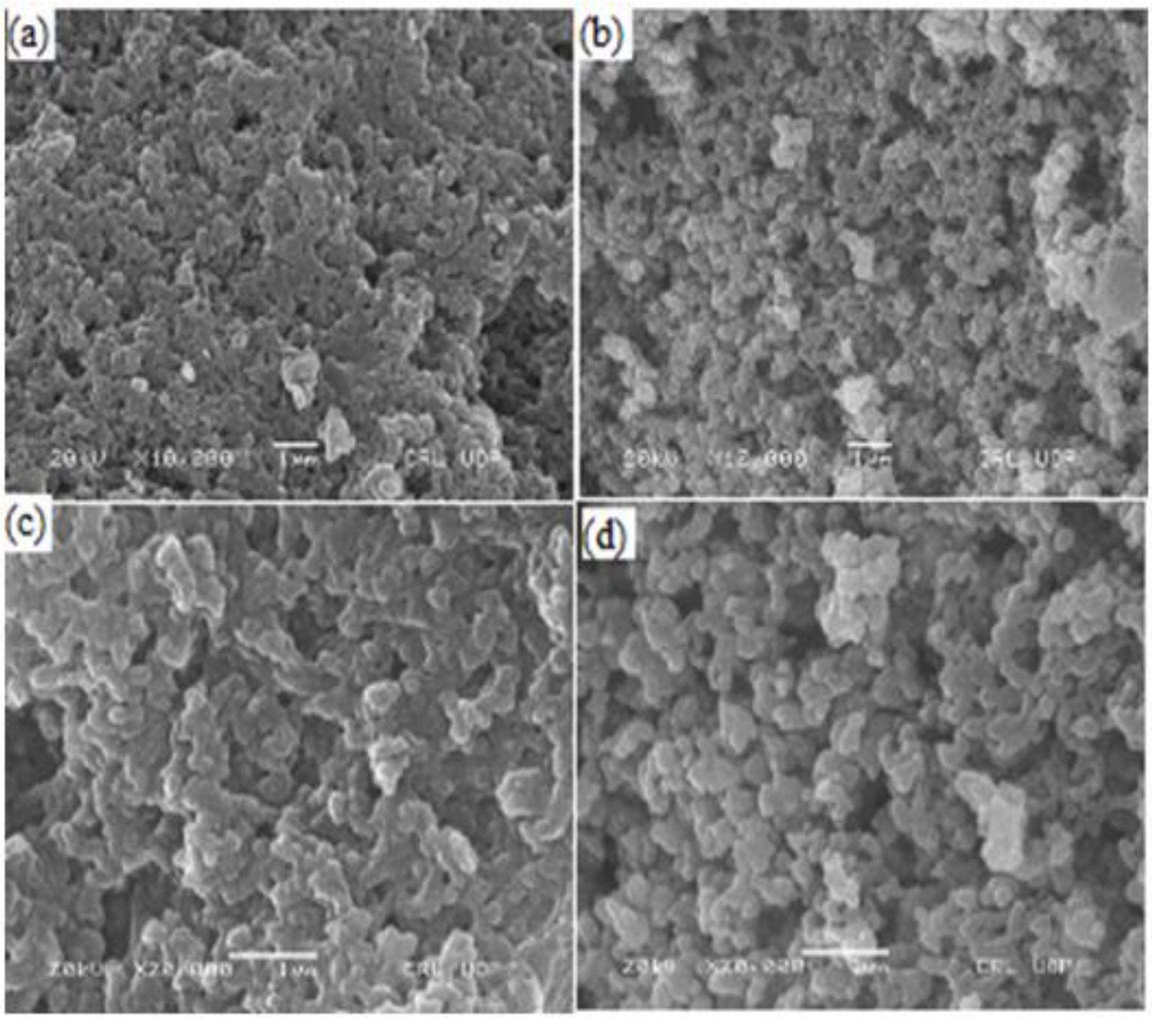

Fig. 4: (a). SEM images of PANI, (b) PANI- TiO_2 composite at lowmagnification , (c) SEM images of PANI and(d) of PANI- TiO_2 composite at high magnification.

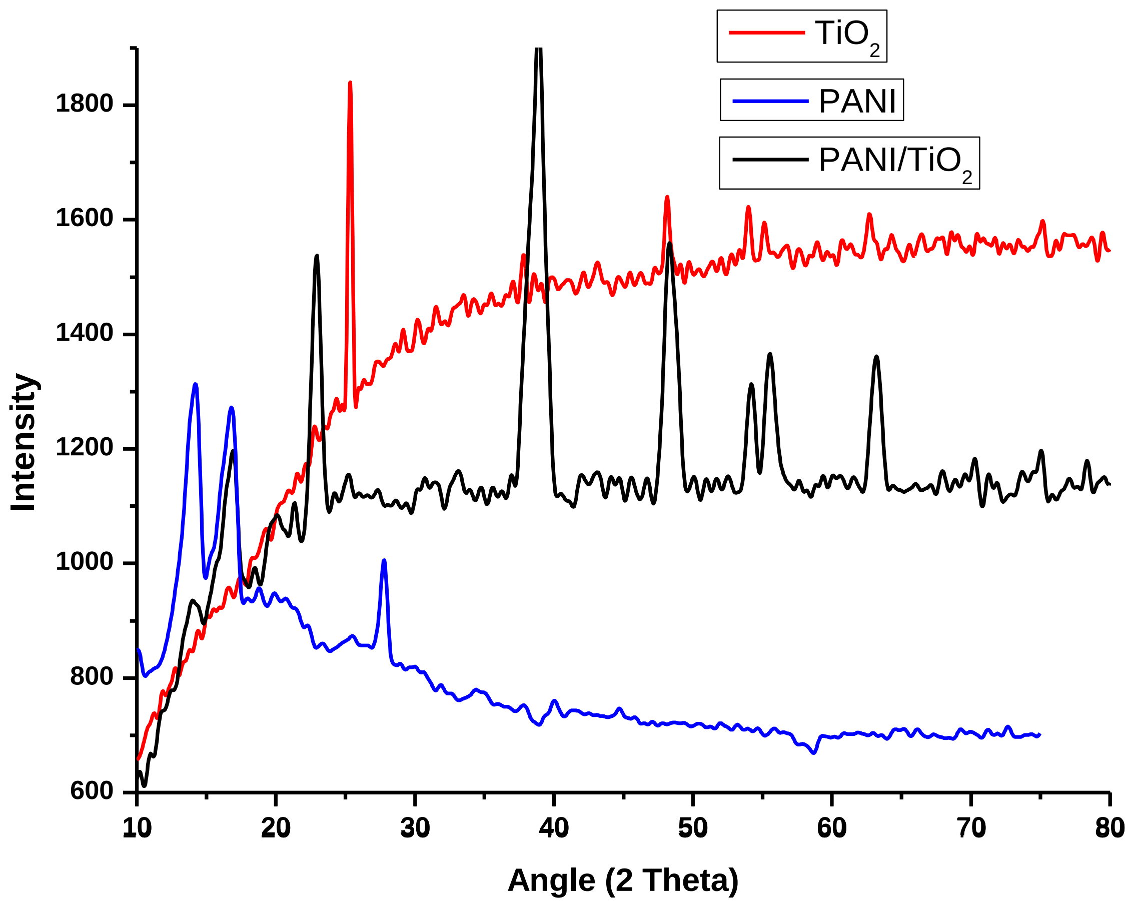

Fig. 5: XRD patterns of TiO_2, PANI and PANI- TiO_2 composite.

FTIR Spectroscopy

FTIR spectra of PANI-TiO_2 composite and PANI are shown in Fig 6. In the FTIR spectrum of PANI, the C=N and C=C stretching modes for the quinoid and benzenoid rings are observed at 1576 and 1485 cm^{-1}respectively. The band at 3230 cm^{-1} is attributed to N-H stretching mode. The band at 1156 cm^{-1} is attributed to an in-plane bending vibration of the C-H bond while the bands at about 1303 and 1236 cm^{-1} ascribed to C-N stretching mode for the benzenoid ring. FTIR spectrum of the PANI-TiO_2 composite indicated contributions from both PANI and TiO_2. The slight shifting in PANI bands are due to the interactions with TiO_2 particles. For example the main characteristic peaks for the composite are observed at 3241, 1553, 1496, 1315, 1236 and 1168 cm^{-1} respectively. The shifting of peaks to higher wavenumber in the composite might be attributed to the strong interaction between the interface of TiO_2 particles and PANI[46]. The shift in the bands of the composite is due to the hydrogen bonding between the N–H groups of PANI and surface of TiO_2 particles [44].

Thermogravimetric Analysis

Thermal stability of PANI and its composites are important for their applications under various thermal conditions. It is observed in Fig 7 that there is a decrease in mass at 200 ˚C which continues up to 750 C˚ for DBSA doped PANI and from 400 ˚C to 650 ˚C for PANI- TiO_2 composite. The release of water molecules from polymer structure is responsible for the initial loss in mass. The loss in mass at higher temperature is due to release of acid dopant from the surface of the polymer chain[34]. The total mass loss up to 800 ˚C was found to be 58% for PANI and 22% for PANI- TiO_2 composite. The TGA analysis shows improved. This comparatively better thermal stability of PANI- TiO_2 composite as compared to PANI is attributed to strong interaction between PANI and TiO_2 interface [44] in the composite.

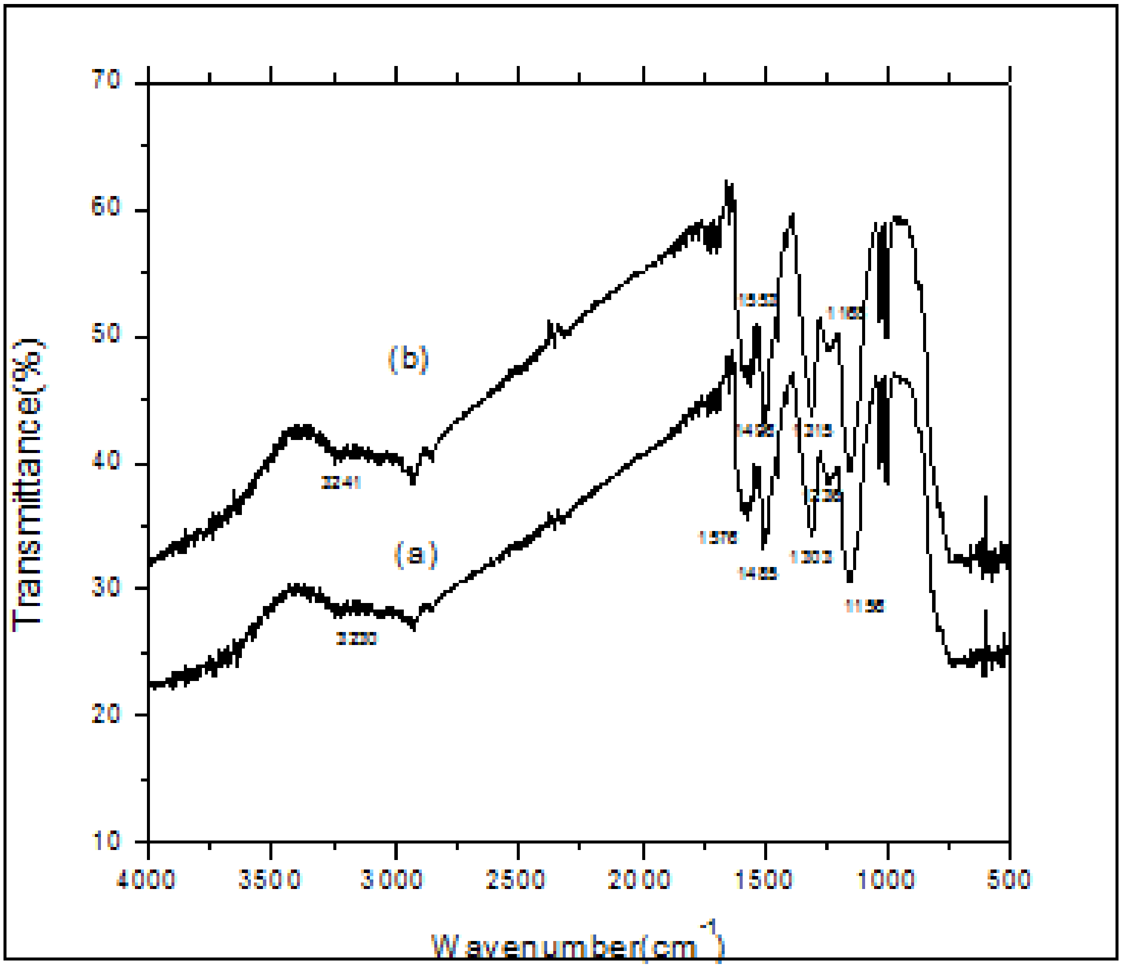

Fig. 6: FTIR spectra of (a) PANI powder and (b) PANI-TiO_2 composite.

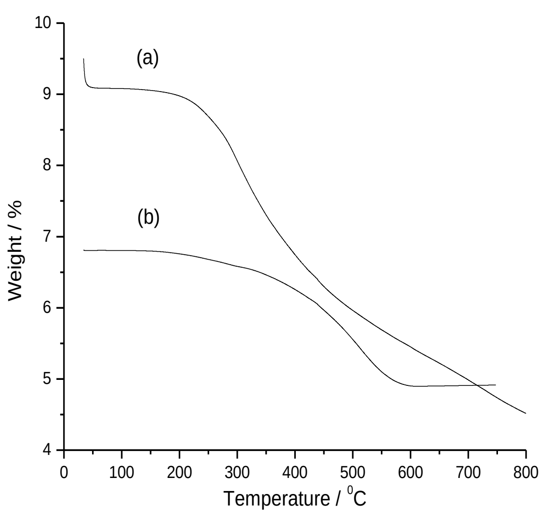

Fig.7: Thermogravimetric curves of (a) PANI and (b) PANI-TiO_2 composite.

Cyclic Voltammetry, Conductivity Measurements and Corrosion Study

Cyclic voltammetry (CV) is a versatile technique for studying electrochemical properties of conducting polymers and other electroactive materials. CVs were recorded in 0.5**M** H_2SO_4 solution in the potential range of -0.20 − 0.90 V at 50 mV/s (Fig. 8). CV curve of PANI shows two anodic peaks on the forward scan. The first anodic peak at 0.25V indicates leucoemeraldine to emeraldine conversion while the 2nd peak at 0.66V indicates further oxidation of emeraldine to pernigraniline. The two cathodic peaks on the reverse scan at 0.62 and 0.003V are assigned to the reduction of pernigraniline into emeraldine and further reduction of emeraldine into leucoemeraldine [47] respectively.

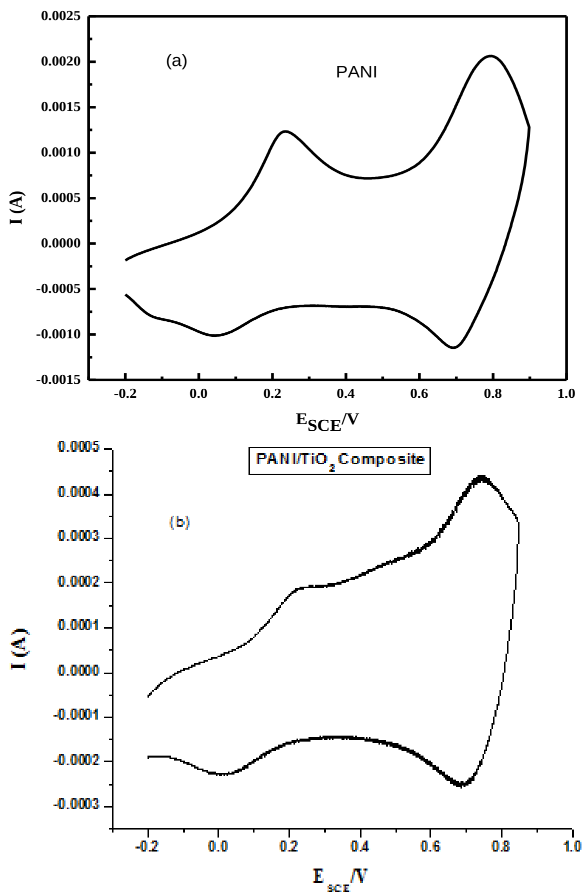

Fig. 8: CVs of (a) PANI and (b) PANI/TiO_2 composite on a gold sheet electrode, in 0.5 M H_2SO_4 at a scan rate of 50 mV/s.

Apparently the CV curve of PANI-TiO_2 composite reflects different picture as compared to the CV of PANI but the number of redox pairs is the same. In the CV of composites the second anodic peak is shifted by 0.08 V towards higher potential. This difference of 80 mV arises from the interaction of TiO_2 with PANI chains in the composite which somehow reduces the rate of oxidation of PANI. This observation can be correlated with the dedoping of PANI-DBSA synthesized in the presence of TiO_2 as observed in the UV-Vis spectroscopy (Fig 3).

Conductivity of the synthesized PANI and PANI-TiO_2 composites was measured with four probe conductivity setup on pressed pellets with Jandel RM3000 test unit. The addition of small amount of TiO_2 resulted in the increase of PANI conductivity. The slight increase with smaller concentration of TiO_2 might be attributed to the extraction of electron from HOMO of TiO_2 and addition into LUMO of PANI because TiO_2 in an n-type and PANI is a p-type semiconductor. However, the conductivity was suppressed with higher concentration of TiO_2 in the polymerization bath. This is attributed to the blockage of the conductive sites of PANI due to agglomeration caused by TiO_2 higher concentration.

The corrosion protection properties PANI-TiO_2 were studied on stainless steel in Indian Ocean water. For the sake of comparison corrosion protection properties of PANI were also studied. The Tafel plots of bare, PANI and PANI-TiO_2 coated steel electrodes are shown in the Fig 9. The resulting calculated values of $E_{corr,}$ i_{corr} and CR mm/year are given in Table-2. The data show that both PANI and PANI-TiO_2 coating cause potential shift and reduction of i_{corr} and CR mm/year of the steel indicating corrosion protection ability of both PANI and the composite. Close observation of Tafel plot shows that potential shift is greater in PANI as compared to its composite. But i_{corr} is reduced to a greater extent in the composite coated electrode as compared to PANI coated electrode. This in turn reduced the corrosion rate to 0.9083 mm/year in the composite coated electrode as compared to 4.007 mm/year in the PANI coated electrode indicating good anticorrosive properties of the composites. Elsewhere a corrosion rate of 0.078 mm/year was reported for the electrochemically prepared PANI-TiO_2 [48] with almost identical corrosion protection efficiency to that of electrochemically synthesized PANI. But the corrosion tests were carried out in 3.5 M NaCl solution. But in our work the corrosion tests were done in complex chemical system of ocean environment.

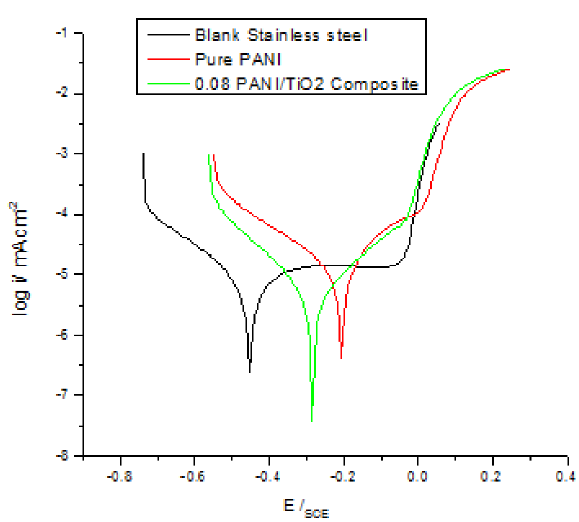

Fig. 9: The Tafel plots of uncoated, PANI and PANI-TiO_2 coated steel electrodes.

Table-2: Corrosion parameters of uncoated, PANI and $PANI-TiO_2$ composite coated stainless steel electrodes.

Parameter	Un coated stainless Steel	PANI coated Stainless Steel	$PANI/TiO_2$ composite coated Stainless Steel
E_{corr}(mV)	-452.0	-207.0	-284.0
i_{corr} (uA/cm^2)	19.90	8.770	1.990
CR (mm/year)	9.072	4.007	0.9083

Conclusions

Soluble $PANI-TiO_2$ composite were prepared successfully through inverse emulsion polymerization method utilizing 2-butanol and chloroform as dispersion media. The synthesized composites were soluble in organic solvents like chloroform, a mixture of toluene and 2-propanol and DMSO. The characterization of $PANI-TiO_2$ composite indicated chemical interaction between the inorganic and organic counter parts of the composite based on UV-Vis and FTIR spectroscopies. Cyclic voltammetry showed good electrochemical activity of $PANI-TiO_2$ composite. The conductivity of PANI was increased with low concentration of TiO_2 but suppressed with higher concentration of TiO_2. The TGA results indicated comparatively higher thermal stability of the composite when compared with PANI. The corrosion protection efficiency of PANI-TiO_2 composites in the Indian ocean water was found to be better than PANI prepared by the same method as well as electrochemically prepared $PANI-TiO_2$ composites reported in the literature.

References

1. R. L. N. Chandrakanthi, M. A. Careem, Preparation and characterization of CdS and Cu_2S nanoparticle/polyaniline composite films, *Thin Solid Films,* **417**, 51 (2002).
2. P. R. Somani, R. Marimuthu, U. Mulik, S. Sainkar and D. Amalnerkar, High piezoresistivity and its origin in conducting polyaniline/TiO_2 composites, *Synth. Met,* **106**, 45 (1999).
3. Y. He, Synthesis of polyaniline/nano-CeO_2 composite microspheres via a solid stabilized emusion route, *Mater.Chem.Phys,* **92**, 134 (2005).
4. P. S. Rao, D. Sathyanarayana, S. Palaniappan, polymerization of aniline in an organic peroxide system by the inverted emusion process, *Macromolecules,* **35**, 4988 (2002).
5. S. AbdulAlmohsin, Z. Li, M. Mohammed, K. Wu and J. Cui, Electrodeposited polyaniline/ multi-walled carbon nanotube composites for solar cell applications, *Synth. Met,* **162**, 931 (2012).
6. J. Wei, S. Xiong, Y. Bai, P. Jia, J. Ma and X. Lu, Polyaniline nanoparticles doped with star-like poly(styrene sulfonate): synthesis and electrochromic properties, *Sol. Energy Mater. Sol. Cells,* **99**, 141 (2012).
7. Y. T. Shieh, J. J. Jung, R. H. Lin, C. H. Yang, T. L. Wang, Electrocatalytic activity of self-doped polyaniline, *Electrochim. Acta*, **70**, 331 (2012).
8. S. W. Phang, M. Tadokoro, J. Watanabe, N. Kuramoto, Synthesis, characterization and microwave absorption property of doped polyaniline nanocomposites containing TiO_2 nanoparticles and carbon nanotubes, *Synth. Met,* **158**, 251 (2008).
9. Y. Li, Y. Huang, S. Qi, L. Niu, Y. Zhang and Y. Wu, Preparation, magnetic and electromagnetic properties of polyaniline/strontium ferrite/multiwalled carbon nanotubes composite, *Appl. Surf .Sci*, **258**, 3659 (2012).
10. L. Liu, F. Tian, M. Zhou, H. Guo and X. Wang, Aqueous rechargeable lithium battery based on polyaniline and LiMn2O4 with good cycling performance, *Electrochi. Acta,* **70**, 360 (2012).
11. F. Chen, P. Liu and Q. Zhao, Well-defined graphene/polyaniline flake composites for high performance supercapacitors, *Electrochim. Acta,* **76**, 62 (2012).
12. Q. Wang, Y. Huang, J. Miao, Y. Zhao and Y. Wang, Synthesis and properties of Li_2SnO_3/polyaniline nanocomposites as negative electrode material for lithium-ion batteries, *Appl. Surf. Sci*, **258**, 9896 (2012).
13. M. Matsuguchi, A. Okamoto, Y. Sakai, Effect of humidity on NH_3 gas sensitivity of polyaniline blend films, *Sensors and Actuators B: Chemical*, **94**, 46 (2003).
14. F. Y. Chuang and S. M. Yang, Titanium oxide and polyaniline core-shell nanocomposites, *Synth. Met,* **152**, 361 (2005).
15. A. Sadek, W. Wlodarski, K. Shin, R. B. Kaner, K. Kalantar-Zadeh, A layered surface acoustic wave gas sensor based on a polyaniline/In_2O_3 nanofibre composite, *Nanotechnology*, **17**, 4488 (2006).
16. S. S. Barkade, J. B. Naik and S. H. Sonawane, Ultrasound assisted miniemulsion synthesis of polyaniline/Ag nanocomposite and its application for ethanol vapor sensing, *Colloids and Surfaces A: Physicochemical and Engineering Aspects*, **378**, 94 (2011).
17. K. Gupta, P. Jana and A. Meikap, Optical and electrical transport properties of polyaniline–silver nanocomposite, *Synth. Met,***160**, 1566 (2010).

18. M. Pavlík, D. Pavliková, L. Staszkova, M. Neuberg, R. Kaliszová, J. Száková, P. Tlustos, The effect of arsenic contamination on amino acids metabolism in *Spinacia oleracea L.*, *Ecotoxicology and environmental safety*, **73**, 1309 (2010).
19. C. Ozdemir, F. Yeni, D. Odaci, S. Timur, Electrochemical glucose biosensing by pyranose oxidase immobilized in gold nanoparticle-polyaniline/AgCl/gelatin nanocomposite matrix, *Food Chem*, **119**, 380 (2010).
20. C. Lai, H. Zhang, G. Li, X. Gao, Mesoporous polyaniline/TiO2 microspheres with core–shell structure as anode materials for lithium ion battery, *J. Power Sources*, **196**, 4735 (2011).
21. X. Ma, M. Wang, G. Li, H. Chen, R. Bai, Preparation of polyaniline–TiO_2 composite film with in situ polymerization approach and its gas-sensitivity at room temperature, *Mater. Chem. Phys*, **98**, 241 (2006).
22. Q. Sheng, M. Wang and J. Zheng, A novel hydrogen peroxide biosensor based on enzymatically induced deposition of polyaniline on the functionalized graphene–carbon nanotube hybrid materials, *Sensors and Actuators B: Chemical*, **160**, 1070 (2011).
23. Y. Zhou, Z. Y. Qin, L. Li, Y. Zhang, Y. L. Wei, L. F. Wang and M. F. Zhu, Polyaniline/multi-walled carbon nanotube composites with core–shell structures as supercapacitor electrode materials, *Electrochim. Acta*, **55**, 3904 (2010).
24. Y. Shimizu, T. Okamoto, Y. Takao and M. Egashira, Desorption behavior of ammonia from TiO2-based specimens—ammonia sensing mechanism of double-layer sensors with TiO_2-based catalyst layers, *J. Mol. Catal. A: Chem*, **155**, 183 (2000).
25. Y. Li;Y. Yu; L. Wu.; J. Zhi. Processable polyaniline/titania nanocomposites with good photocatalytic and conductivity properties prepared via peroxo-titanium complex catalyzed emulsion polymerization approach, *Appl.Surf. Sci*, **273**, 135 (2013).
26. S. Sathiyanarayanan, S. S. Azim and G. Venkatachari, A new corrosion protection coating with polyaniline–TiO_2 composite for steel, *Electrochim. Acta*, **52**, 2068 (2007).
27. C. Bian;Y. Yu.;G. Xue. Synthesis of conducting polyaniline/TiO_2 composite nanofibres by one-step in situ polymerization method *J. Appl. Polym. Sci*, **104**, 21 (2007).
28. W. Feng, E. Sun, A. Fujii, H. Wu, K. Niihara, K. Yoshino, *Bull.* Synthesis and characterization of photoconducting polyaniline-TiO_2 nanocomposite, *Chem. Soc. Jpn*, **73**, 2627 (2000).
29. D. C. Schnitzler, A. J. Zarbin, Organic/inorganic hybrid materials formed from TiO2 nanoparticles and polyaniline, *J. Brazilian Chemical Society*, **15**, 378 (2004).
30. H. Xia and Q. Wang, Ultrasonic irradiation: a novel approach to prepare conductive polyaniline/nanocrystalline titanium oxide composites, *Chem. Mater*, **14**, 2158 (2002).
31. J. E. Osterholm, Y. Cao, F. Klavetter and P. Smith, Emulsion polymerization of aniline, *Polymer*, **35**, 2902 (1994).
32. P. J. Kinlen, J. Liu, Y. Ding, C. R. Graham, E. E. Remsen, Emulsion Polymerization Process for Organically Soluble and Electrically Conducting Polyaniline, *Macromolecules*, **31**, 1735 (1998).
33. S. Bilal, S. Gul and K. Ali, Synthesis and characterization of completely soluble and highly thermally stable PANI-DBSA salts, *Synth. Met*, **162**, 2259 (2012).
34. M. R. Karim, H. W. Lee, I. W. Cheong, S. M. Park, W. Oh, J. H. Yeum, Conducting polyaniline-titanium dioxide nanocomposites prepared by inverted emulsion polymerization, *Polym. Compos.* **31**, 83 (2010).
35. S. Shreepathi and R. Holze, Spectroelectrochemical investigations of soluble polyaniline synthesized via new inverse emulsion pathway, *Chem Mater*, **17**, 4078 (2005).
36. P. Ghosh, S. K. Siddhanta, S. R. Haque and A. Chakrabarti, Stable polyaniline dispersions prepared in nonaqueous medium: synthesis and characterization, *Synth. Met*, **123**, 83 (2001).
37. Y. Guo, D. He, S. Xia, X. Xie, X. Gao and Q. Zhang, Preparation of a novel nanocomposite of polyaniline core decorated with anatase-TiO_2 nanoparticles in ionic liquid/water microemulsion, *J. Nanomaterials*, **2012**, 8 (2012).
38. Y. Cao, P. Smith, A. J. Heeger, Counter-ion induced processibility of conducting polyaniline and of conducting polyblends of polyaniline in bulk polymers, *Synth.Met*, **48**, 91(1992).
39. L. Dai, J. Lu, B. Matthews, A. W. Mau, Doping of conducting polymers by sulfonated fullerene derivatives and dendrimers. The Journal of Physical Chemistry B, *J. Phy. Chem. B*, **102**, 4049(1998)
40. A. L. Schemid, S. I. Torresi, A. N. Bassetto, I. A. Carlos, Structural, morphological and spectroelectrochemical characterization of poly (2-ethyl aniline), *Journal of the Brazilian Chemical Society*, **11,** 317 (2000).
41. M. Omastová, K. Mosnáčková, M. Trchová, E. N. Konyushenko, J. Stejskal, P. Fedorko, J. Prokeš, Polypyrrole and polyaniline prepared

with cerium (IV) sulfate oxidant, *Synth. Met*, **160**, 701 (2010).

42. I. Sapurina, J. Stejskal, The mechanism of the oxidative polymerization of aniline and the formation of supramolecular polyaniline structures, *Polym. Int,* **57**, 1295 (2008).
43. S. Pawar, S. Patil, M. Chougule, S. Achary, V. Patil, Microstructural and optoelectronic studies on polyaniline: TiO_2 nanocomposites, *Int.J. Polymer Mater*, **60**, 244(2010).
44. X. Li, W. Chen, C. Bian, J. He, N. Xu, G. Xue, Surface modification of TiO_2 nanoparticles by polyaniline, *Appl. Surf. Sci*, **217**, 16 (2003).
45. S. Pawar, S. Patil, M. Chougule, B. Raut, P. Godase, R. Mulik, S. Sen, V. Patil, New Method for Fabrication of CSA Doped PANi-TiO_2 Thin-Film ,Ammonia Sensor, *IEEE Sens. J*, **11**, 2980 (2011).
46. T. Ozawa. Estimation of activation energy by isoconversion methods, *Thermochim Acta*, **203**, 159 (1992).
47. S. Bilal, S. Gul, R. Holze, An impressive emulsion polymerization route for the synthesis of highly soluble and conducting polyaniline salts, *Synth. Met*, **206**, 131 (2015).
48. M. Ates and E. Topkaya, Nanocomposite film formations of polyaniline via TiO_2, Ag and Zn and their corrosion protection properties, *Prog. Org. Coat*, **82**, 33 (2015).